PROCEEDINGS, 43rd Workshop on Geothermal Reservoir Engineering
Stanford University, Stanford, California, February 12-14, 2018
SGP-TR-213

Geothermal Exploration in the Vicinity of Wells, Nevada

Nicolas Spycher[1*], Richard E. Zehner[2], Andrew Zuza[3], Markus Bill[1], Bridget Ayling[4], Richard Hammack[5], Garret Veloski[5], Mark McKoy[6*], Emily Cameron[7], C. Gabe Creason[7], Jennifer DiGiulio[7], Patrick Dobson[1], Devin Justman[7], Roy Miller[7], Mackenzie Mark-Moser[7], Kelly Rose[7], Drew Siler[8], Ira Rackley[9], Jolene Supp[10], Kelby Bosshardt[11]

[1] Lawrence Berkeley National Laboratory, Berkeley, CA, USA
[2] Lumos and Associates, Reno, NV, USA
[3] Nevada Bureau of Mines and Geology, University of Nevada, Reno, NV, USA
[4] Great Basin Center for Geothermal Energy, University of Nevada, Reno, NV, USA
[5] National Energy Technology Laboratory, Pittsburgh, PA, USA
[6] National Energy Technology Laboratory, Morgantown, WV, USA
[7] National Energy Technology Laboratory, Albany, OR, USA
[8] U.S. Geological Survey, Menlo Park, CA, USA
[9] Elko Heat Company, Elko, NV, USA
[10] City of Wells, Wells, NV, USA
[11] Better City, Ogden, UT, USA

*Principal Investigators; nspycher@lbl.gov, mark.mckoy@netl.doe.gov

Keywords: Direct Use, Geochemistry, Geophysics, Structural, Geothermometry, GIS, Conceptual Model, Basin and Range

ABSTRACT

Geothermal activity in and around the City of Wells, Nevada, is evidenced by hot springs and the presence of hot waters in several private and municipal wells, suggesting that this area may host a commercially-viable geothermal resource. For this reason, under the U.S. Department of Energy's Small Business Vouchers Pilot (SBV) Program, research teams from Lawrence Berkeley National Laboratory (LBNL) and the National Energy Technology Laboratory (NETL), in collaboration with the University of Nevada, Reno (UNR), worked closely with the Elko Heat Company, the City of Wells, and Better City to review existing data and conduct field studies to site a geothermal well for district heating and other direct use applications for the Wells community. This effort started with the compilation and review of existing structural, geochemical, and geophysical information for this area. New field investigations included the measurement of ground temperatures with shallow 2-meter probes and in deeper Geoprobe holes, the collection and geochemical analysis of water samples from springs and wells, geologic mapping, direct current (DC) ground resistivity surveys, and electromagnetic induction (EMI) surveys. These data were integrated into a GIS geodatabase and a 3D conceptual geological model. A zone of anomalously high temperatures at shallow depths was identified in an area that coincides with the possible intersection of N-S and E-W faults. This zone exhibits low electrical resistivity in the shallow subsurface (depths less than 50 m), suggesting the presence of hot subsurface fluids at this location. While no subsurface waters have been sampled in this area, water samples from springs and wells to the east and west of this zone were found to display differing chemical and isotopic characteristics, suggesting that this zone may be related either to outflow from the hot spring system northwest of the City, or to outflow from a blind system further east following the regional hydraulic gradient. Maximum temperatures for the two groups of these fluids estimated by multicomponent geothermometry are ~180°C for the hot spring system and ~160°C east of the shallow temperature anomaly. The drilling of exploration wells at recommended locations within the temperature anomaly and other areas deemed favorable has provided additional information on the potential for shallow (less than 150 m deep) and deeper resources of hot water for direct use by the community of Wells.

1. INTRODUCTION

The City of Wells, Nevada has hot springs, thermal wells and a geologic setting conducive to hosting a viable geothermal resource. For this reason, the City of Wells reached out to Elko Heat Company (EHC) for assistance in determining economic opportunities using geothermal heat nearby. EHC was formed in 1979 as a municipally-owned entity in response to a United States Department of Energy (U.S. DOE) program opportunity notice to promote the use of geothermal resources. Now EHC is a privately held utility that has provided geothermal heat through a district heating system to the central business district of Elko, Nevada, a geothermal industrial park, and adjoining residential areas (Bloomquist, 2004).

Under the U.S. DOE Small Business Vouchers (SBV) Pilot Program, EHC and City of Wells worked closely with research teams from Lawrence Berkeley National Laboratory (LBNL) and the National Energy Technology Laboratory (NETL), in collaboration with the University of Nevada Reno (UNR), to improve the current understanding of the geothermal system(s) around Wells with the objective to identify a source of geothermal fluids ≥ ~65°C for district heating, in lieu of electricity currently used for heating systems, which would result in cost savings and reduce greenhouse gas emissions.

2. APPROACH

This study involved the review of existing information and collection of new data to refine the Wells geothermal resource models originally developed by Jewell (1982) and Jewell et al. (1994). A multipronged approach was implemented, consisting of: 1) the collection and synthesis of existing geologic, geochemical, geophysical, and hydrologic data for the Wells area; 2) a review and analysis

of existing and newly collected geochemical data from wells and springs to assess the origins and deep temperatures of fluids; 3) structural mapping and the development of a structural model for the Wells geothermal system; 4) the collection of additional field data including 2-meter shallow probe and deeper Geoprobe temperature surveys, and electromagnetic induction (EMI) induction and direct current (DC) resistivity surveys. A conceptual geologic model for the Wells geothermal system was then developed on the basis of these data. This involved integrating relevant datasets (historical and new) into EarthVision, a software package used for analysis, visualization, and 2- and 3-dimensional modeling of spatially referenced data. The completed model was used to visualize geologic and geothermal trends in the subsurface, identify regions of highest density and/or quality data, and inform decision-making on optimal location(s) for one or more geothermal exploration wells. These various investigations are summarized below, with emphasis on the geochemical exploration part of this study. A project report including all gathered historical and new data, and their analysis, is currently in preparation and will be made available through LBNL and NETL.

3. GEOLOGIC SETTING AND HYDROTHERMAL ACTIVITY

The City of Wells lies in the Basin and Range Province in northeast Nevada (Figure 1). The geology of this area is dominated by outcrops of Paleozoic rock in the Ruby, Snake, and Humboldt Mountains, and mostly Miocene sediments and tuffs in the Elko Basin to the west and Town Creek Flat Basin to the northeast (Ponce and Bouligand, 2011). Underlying these basins is the pre-Cenozoic basement, which deepens to over 5 kilometers in the Elko Basin, shallows significantly eastward toward Wells, deepens to about 1.8 kilometers to the northeast in the Town Creek Flat Basin, and outcrops in the surrounding mountain ranges (Ponce and Bouligand, 2011).

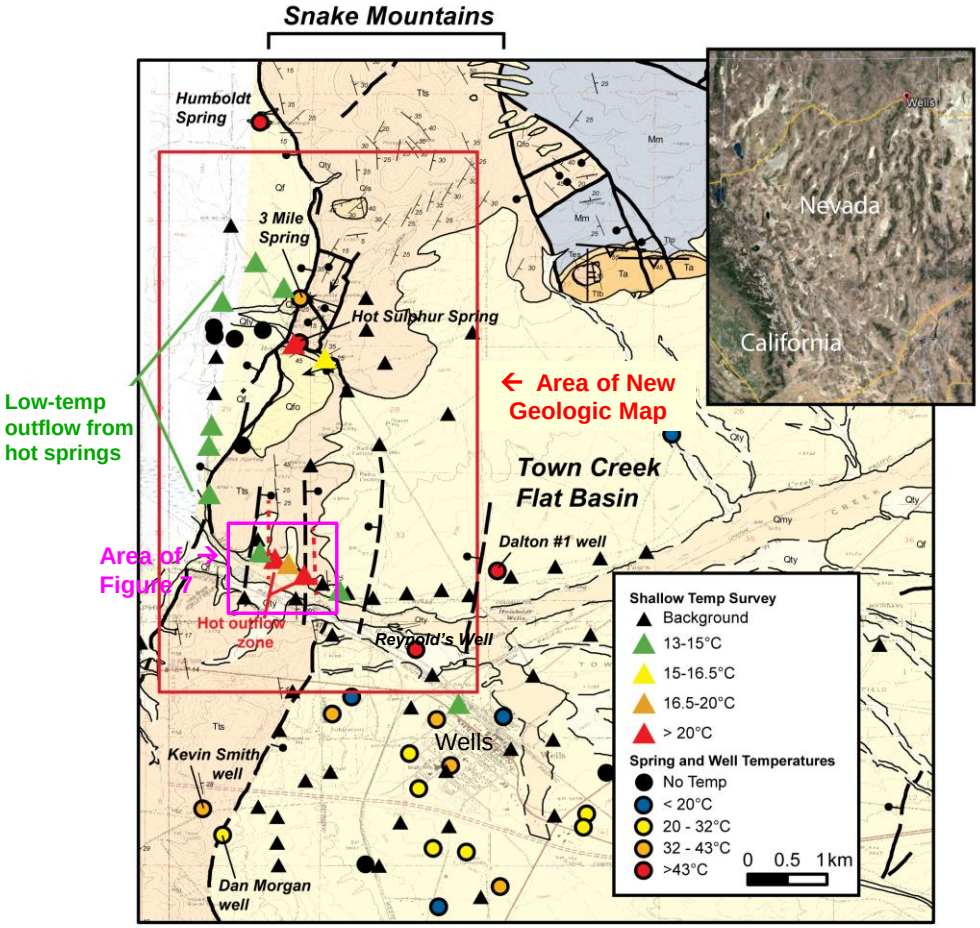

Figure 1. Map of the southern Snake Mountains showing the local geology (Henry and Thorman, 2011), locations of wells and springs and their temperatures (Jewell, 1982), as well as result from a new shallow temperature survey with inferred geothermal outflow zones (Zehner, 2016; soil temperatures above ~13°C background). Inset shows the location of the City of Wells, Nevada, on a Google Earth map.

Previous geologic maps completed near Wells and the surrounding regions include those of Garside (1968), Jewell (1982), Thorman et al. (2010), and Henry and Thorman (2011). In addition, a more refined geologic map was completed for this study by UNR (Zuza, 2017) covering the area outlined on Figure 1. The north-trending Snake Mountains are located to the northwest of Wells. Volcanic and sedimentary rocks from the Miocene Threemile Spring unit are dominant in the southern portion of this range (Garside, 1968). These

strata are observed unconformably overlying the Mississippian Melandco sandstone (Henry and Thorman, 2011). Along the Snake Mountains, sedimentary rock layers are tilted moderately (~25°) to the east. Quaternary normal faults are observed along the western flank of the Snake Mountains and within the Town Creek Flat Basin. These faults are predominately west-dipping, but older variably dipping faults have been reported along the eastern flank of the Snake Mountains (Jewell, 1982; Thorman et al., 2010; Ramelli and DePolo, 2011). Due to relatively poor exposures in hills around Wells, the best observations of the local stratigraphy come from cuttings from an older oil exploration well (Dalton #1) located within the study area (Figure 1) (Jewell, 1982). The overall lithology encountered by this well consists of siltstone, tuffaceous siltstone, sandstone, and conglomerate (poorly sorted clasts of volcanics, quartzite, siltstone, and chert cobbles) that are poorly sorted. Along the eastern side of the range-bounding normal fault, silicification occurs within the Threemile Spring unit and is most obvious within one (or several) conglomerate unit(s) (Jewell, 1982; Zehner, 2016). Following a shallow temperature survey conducted for this study, Zehner (2017a) suggests that geothermal fluids likely flow up along the western range-bounding normal fault and outflow along the east-southeast-dipping conglomerate strata (Figure 1). The exact path of these fluids is not known, but these observations highlight that past and present geothermal-fluid flow may be controlled by the geometries of the dipping Miocene strata, the west-dipping normal faults, and any silicified structures. Two possible conceptual models of thermal water flow in the area are illustrated in Figure 2.

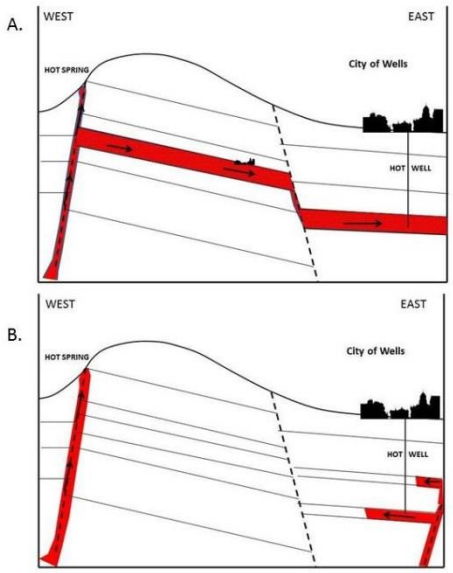

Figure 2. – Two conceptual models for upflow zones feeding hot springs and warm wells around the City of Wells, Nevada (from Zehner, 2016, after Jewell, 1982).

It should be noted that in 2008 a magnitude 6.0 earthquake occurred 9 km northeast of the town of Wells (Smith et al., 2011; Sladek, 2011; Henry and Colgan, 2011). Although mapped faults did not have noticeable movement, the temperature of water in wells and springs in and around town increased up to 9ºC, and the clarity of water decreased temporarily in some wells. These observations suggest that wells and springs in the area may be hydraulically connected to faults that experienced at least small amounts of slippage.

4. WATER GEOCHEMISTRY AND SOLUTE GEOTHERMOMETRY

Existing geochemical analyses of water samples from springs (hot and cold) and wells around the City of Wells were compiled from a review of available published papers and reports, including those of Garside and Schilling (1979), Garside (1994), Jewell (1982), Jewell et al. (1994 and personal communication), Sladek et al. (2011), and Zehner (2016). These data also included analyses compiled by the Nevada Bureau of Mines and Geology (NBMG). To complement these historical water chemistry data, a field sampling survey was conducted by LBNL and UNR in April 2017, covering an area from Humboldt Springs to the North, to Railroad Spring South of Wells (Figure 3). During this time, 7 city wells, 6 private wells, 3 cold springs and 3 hot springs were sampled for general chemical and C, O, H isotopic compositions. Sampled hot springs included Threemile and Humboldt springs. Hot Sulphur Spring (Figure 1) reportedly dried out after the 2008 earthquake, while at the same time flow increased at Threemile spring (Bottari, personal communication). Later in the Summer 2017, the City of Wells provided samples from 3 water wells northeast of town, and also from Twelvemile Spring, a thermal feature outside our area of direct interest about 20 km north of town. In August 2017, 11 more samples were collected by NETL from ground-water seeps within the floodplain of the Humboldt River to the northwest of Wells. Two other samples from one location in the Humboldt River were also collected by LBNL in October 2017.

Samples from April 2017 were collected either directly from sampling ports on well heads or using a peristaltic pump, and a syringe with in-line 0.2 micron filters to minimize contact with air. The water pH, electrical conductivity, and chloride concentration (Quantab) were measured in the field. Collected samples were analyzed in the laboratory for metals by ICP-MS, anions by IC, TIC-TOC (total

inorganic and total organic carbon) by infrared analyzer, as well as C, O and H isotopic composition. Samples collected after April 2017 were taken without preservation or filtration and were analyzed only for their isotopic composition.

Both the newly acquired and previously reported geochemical data were evaluated to provide insights on the origin of sampled waters and possible geothermal reservoir temperatures. This effort included traditional graphical analyses such as correlation plots, principal component analyses (PCA), the application of various traditional solute geothermometers, and multicomponent geothermometry computations using the iGeoT software (Spycher et al., 2014; 2016). In general, the new analytical results were found to be consistent with previously reported data for major constituents. Trace element data were, for the most part, not reported in previous studies.

Thermal waters in the vicinity of Wells can be characterized as sodium-bicarbonate waters with low chloride concentrations typically between about 10 and 40 mg/L. Waters with the highest total dissolved solids (around 2000 mg/L, primarily as bicarbonate with up to about 400 mg/L sodium) occur at Threemile and Humboldt hot springs, where thermal waters are found to also have the highest temperatures (between about 40 and 60°C) compared to other sampled waters in the Wells area. Colder waters typically have higher proportions of calcium and magnesium (up to about equal proportions with sodium on an equivalent basis), and lower chloride concentrations (Figure 4, left). Two samples (at one location) from the Humboldt River collected in October 2017 (#36 and #37) and one sample collected by Jewell et al. (1994) near this river (#51) showed significantly higher chloride concentrations (> 100 ppm) presumably from evaporative concentrations along this non-perennial river.

ID	Name	Type	Date Sampled	Temp (°C)
1	Rural Electric	City Well	4/26/2017	34.6
2	Well #2	City Well	4/26/2017	29.0
3	Well #6	City Well	4/26/2017	26.0
4	Golf Course Well	City Well	4/26/2017	23.3
5	Well #7	City Well	4/26/2017	20.9
6	Well #5	City Well	4/26/2017	25.4
7	Airport Well	City Well	4/26/2017	13.5
8	Reynolds Well	Private Well	4/26/2017	41.0
9	Arnold Merrill Well	Private Well	4/27/2017	20.1
10	BTI Well	Private Well	4/27/2017	30.5
11	Dan Morgan Well	Private Well	4/27/2017	32.0
12	Reynolds House	Private Well	4/28/2017	17.7
13	Bottari Well	Private Well	4/28/2017	21.4
14	Three-mile spg	Spring	4/27/2017	41.6
15	Humboldt spg (lower)	Spring	4/27/2017	53.0
16	Humboldt spg (upper)	Spring	4/27/2017	44.9
17	Spring (NID 20)	Spring	4/28/2017	16.2
18	Railroad Spg	Spring	4/28/2017	23.7
19	"Last" Spring**	Spring	4/28/2017	15.0
20	Twelve-mile spg (hot)*	Spring	June 2017	
21	Twelve-mile spg (colder)*	Spring	June 2017	
22	Trap Range Well*	Private Well	June 2017	
23	Windmill Well*	Private Well	8/30/2017	
24	Ritchie's Well*	Private Well	8/30/2017	
25	Seep 1*	Seep/spring	August 2017	17.0
26	Seep 2*	Seep/spring	August 2017	13.5
27	Seep 3*	Seep/spring	August 2017	17.2
28	Seep 4*	Seep/spring	August 2017	
29	Seep 5*	Seep/spring	August 2017	22.6
30	Seep 6*	Seep/spring	August 2017	18.0
31	Seep 7*	Seep/spring	August 2017	15.9
32	Seep 8*	Seep/spring	August 2017	
33	Seep 9*	Seep/spring	August 2017	15.4
34	Seep 10*	Seep/spring	August 2017	16.4
35	Seep 11*	Seep/spring	August 2017	16.4
36	E_Fork Humboldt River a*	River	10/1/2017	8.2
37	E_Fork Humboldt River b*	River	10/1/2017	8.2

* Samples collected in soda bottles without preservation or filtration – isotopic analyses
** Arbitrary name chosen for this study

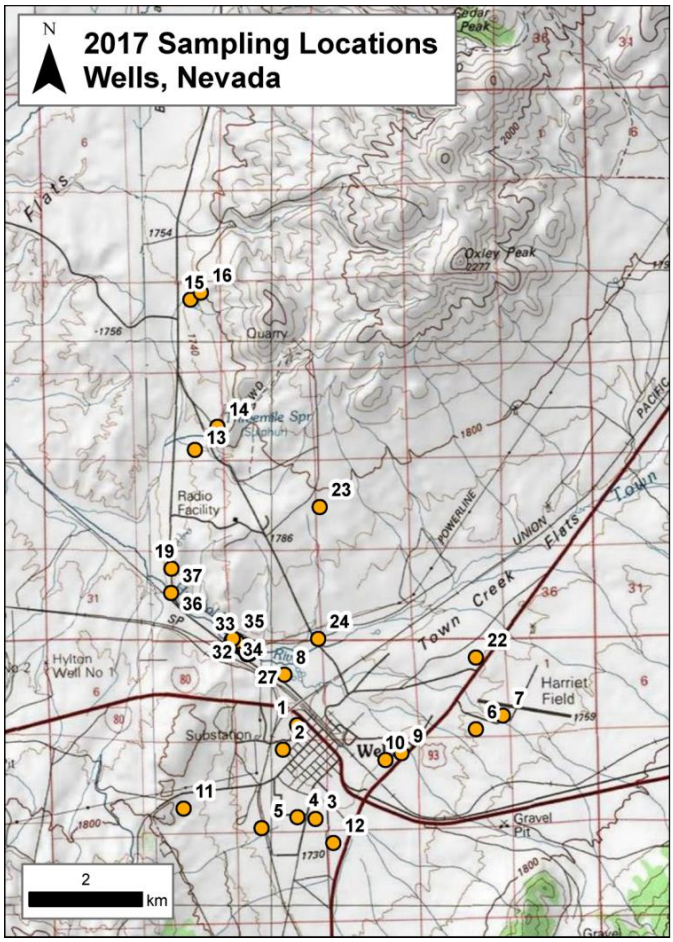

Figure 3. Locations of water samples collected for chemical and isotopic analysis. Note that three samples fall outside the map: Railroad Spring (#18) is located about 4 km south of Wells, around one km west of Old Clover Valley Road; and Twelve-mile hot spring (#20 and #21) is located about 20 km north of Wells along Bishop Creek.

Previous studies using Piper diagrams suggested that mixing occurs between cold waters in the Wells area and the hot spring waters from Threemile and Humboldt hot springs to the northwest of the city (Jewell et al., 1994). While such a mixing trend could be implied by looking only at major chemical parameters on a Piper diagram (Figure 4, left), a closer examination of all geochemical data (including trace metal and isotopic analyses not previously available) show that waters along, and to the west of, the western Snake Mountain range-bounding fault have distinct chemical signatures from waters east of this boundary. Indeed, the waters west of the fault show remarkably higher concentrations of sodium and bicarbonate when compared to the other waters (Figure 4, right). These include samples from the hot springs (#14, Threemile; #15 and #16, Humboldt), a sample from the Bottari well downgradient and west of the hot springs (#13), and a cold spring sample collected 1.5 to 3 km south-southwest of the hot springs at a location near the Snake Mountain range-bounding fault (#19, Last Spring). All historical data from these areas show the same trend of elevated sodium and bicarbonate concentrations compared to other waters sampled east of the range-bounding fault. These two distinct groups are hereafter referred to as the "Northwest Group" (elevated sodium and bicarbonate) and the "East" Group (lower sodium and bicarbonate than the Northwest Group).

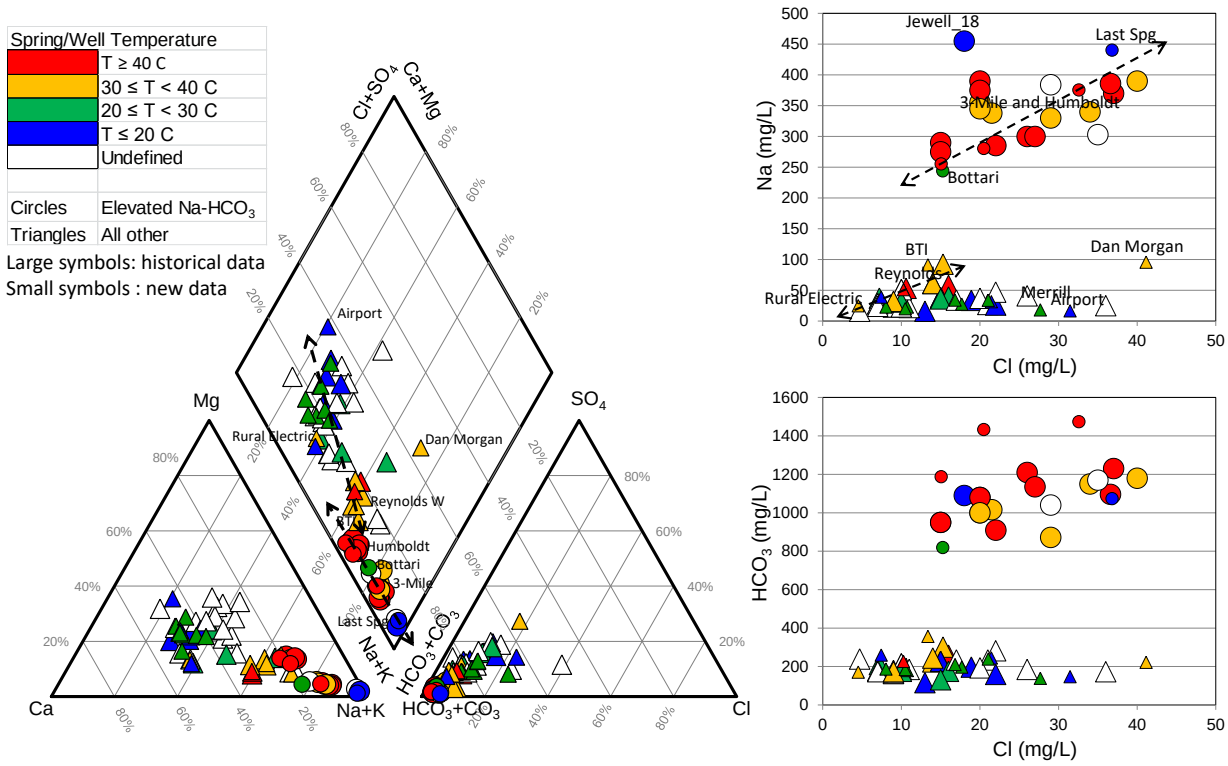

Figure 4. Piper diagram (left) showing new (small symbols) and previously published analyses (large symbols) of thermal and non-thermal waters in the vicinity of Wells. A close examination of these data (right) reveals two groups of waters: those with elevated sodium and bicarbonate (high Na and HCO_3, shown with circles, Northwest Group), and those with lower concentrations of these solutes (shown with triangles, East Group), with each group displaying its own separate mixing trend rather than one global mixing trend for all waters. Symbols colors indicate temperature as shown on the legend. Arrows indicate possible mixing trends.

The distinction between the Northwest and East groups of waters is also clear when looking at the concentration of trace elements such as boron (B), lithium (Li), cesium (Cs), rubidium (Rb), and germanium (Ge) (Figure 5). The fact that these elements show a significant enrichment in waters from the Northwest Group compared to the East Group, and significantly higher Ge/Si ratios (e.g., Evans and Derry, 2002), in addition to elevated bicarbonate concentrations, could point to an origin that is associated with stratigraphically deeper carbonate and/or igneous rocks, in contrast with shallower clay-rich alluvial/fluvial deposits. An origin from deep rocks is also consistent with the association of hot springs with a range-bounding fault. In contrast, waters from the East Group could have been depleted in lithium and cesium while interacting with more clay-rich sedimentary rocks and also be depleted in boron and germanium because of a shallower, cooler origin or a greater distance from a deep source.

The isotopic compositions of the Northwest and East Groups of waters further show the distinction between these two groups of waters (Figure 6). Waters from the East Group fall more-or-less aligned with, or close to, the line established for local meteoric waters in a climatic environment similar to that of Wells (Idaho Falls rain), suggesting an origin from recharge of rainfall (Figure 6, left). In contrast, waters from the Northwest Group are isotopically shifted to higher $\delta^{18}O$ values. Such a shift in waters in the Great Basin has been considered a possible indication of Pleistocene waters (Smith et al., 2002), which would imply a deeper origin. The O-H composition of the seeps (points #25 to #35 in Figure 3) appear to follow an evaporation trend from the line defining the East Group

waters towards the Humboldt River samples, consistent with the fact that these surface seeps were sampled during summer when surface evaporation was high, and also consistent with the trend of surface water data in a similar environment (Eastern Snake River Plain).

The carbon isotopic compositions, when plotted against dissolved inorganic carbon (DIC) concentrations (in this case essentially all bicarbonate), also show distinct trends for the Northwest and East Groups of waters (Figure 6, right). The $\delta^{13}C$ values are higher and DIC concentrations more elevated in the Humboldt and Threemile hot springs, which could reflect dissolution of deep Paleozoic limestones and/or metamorphosed carbonates at depth. The trend of decreasing DIC values and slightly increasing $\delta^{13}C$ values away from the hot springs could be compatible with progressive degassing of CO_2 from these waters as they outflow away from the range-bounding fault towards the Bottari well. In contrast, the much lower $\delta^{13}C$ values and lower DIC concentrations that define the trend of the East Group waters could imply they are associated with biogenically derived CO_2, at the lower end of the trend, mixing with degassed waters originating from a source similar to the NW Group waters. Because the BTI well (#10, Figure 3) plots closer to the hypothetical mixing point (where the dashed lines would cross on Figure 6, right) but is located much farther east of the hot spring area than the Reynolds (#8) or Rural Electric wells (#1, Figure 3), we suggest that the thermal component of the East Group waters is not likely to originate from waters feeding the hot springs. Rather, East Group waters appear more likely to originate from fluids that initially follow a similar chemical evolution as the hot spring fluids at depth, but at a different location further east along one or more concealed faults. These fluids would then migrate through clay-rich sediments, lose their deeper trace element signature, degas and mix with shallower ground waters. This would correspond to a conceptual model similar to that illustrated in Figure 2B. Unfortunately, the lack of data on the depth of water production zones and/or the large perforated intervals in many wells precludes a thorough analysis of spatial concentration trends. However, it is interesting that even without depth-resolved data, isotopic trends for these waters show well-defined and remarkably different trends in the Northwest and East Groups.

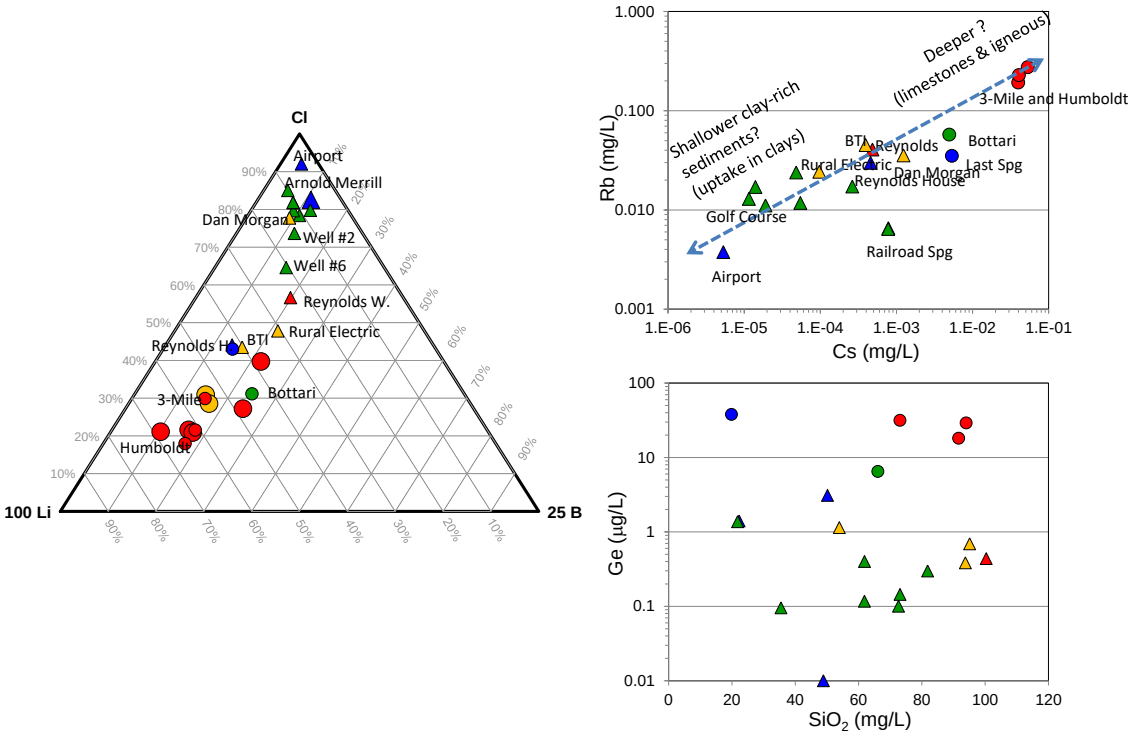

Figure 5. Ternary and binary plots of trace elements and silica showing the distinct compositions of waters from the Northwest Group (circles) and East Group (triangles). Symbols colors indicate temperature as shown in the legend of Figure 4.

Reservoir temperatures were estimated using various solute geothermometry approaches with chemical analyses from previous studies and new samples. New and previously reported chemical analyses were found to be fairly consistent, thus yielding similar reservoir temperatures. Classical geothermometers were found to give inconsistent results among both the thermal and cold waters. This has been observed with waters from the Basin and Range province because of re-equilibration, equilibration with minerals different from those on which classical geothermometers rely, and/or dissolution of salts in the shallow subsurface that mask the chemical signature of deep reservoirs (e.g. Peiffer et al., 2014). For waters with discharge temperatures above 30°C, the highest temperatures were obtained with the Na/K geothermometer (~230°C and above) and lowest temperatures with the K/Mg geothermometer (~100°C). The silica-quartz (conductive) temperatures of the thermal waters fall for the most part between 120 and 140°C; these values assume no dilution and

would be higher if mixing occurred with cold ground waters with lower silica concentrations. When plotted on a Giggenbach ternary Na-K-Mg geothermometer diagram, all samples are found to fall within the field of waters considered "immature" (Giggenbach, 1988), for which the application of classical geothermometers is not recommended.

Multicomponent geothermometry computations with iGeoT were carried out in an attempt to narrow the range of estimated reservoir temperatures. This method relies on the saturation indices of multiple minerals and complete analyses of water samples (Reed and Spycher, 1984). Numerical optimization with iGeoT allows for the reconstruction of deep water compositions to account for effects of mixing, degassing, and/or reactions that are not necessarily those on which classical geothermometers are based. With the hot spring samples, reservoir temperatures around 180°C were obtained assuming quartz, calcite, K-feldspar and Na-montmorillonite as minerals at or near equilibrium with the deep reservoir fluid, little dilution (~9%) and only small amounts of CO_2 degassing. For the Reynolds and BTI wells (with highest temperature discharge), somewhat lower temperatures in the 160°C range were obtained using the same minerals however with more dilution (~ 50%). It should be noted that higher temperatures could also be computed using higher dilution factors and/or other minerals, although with worse fits. Furthermore, these temperatures were calculated using measured aluminum (Al) concentrations, which could be underestimated if Al dropped from solution upon cooling. In such case computed temperatures would also be underestimated.

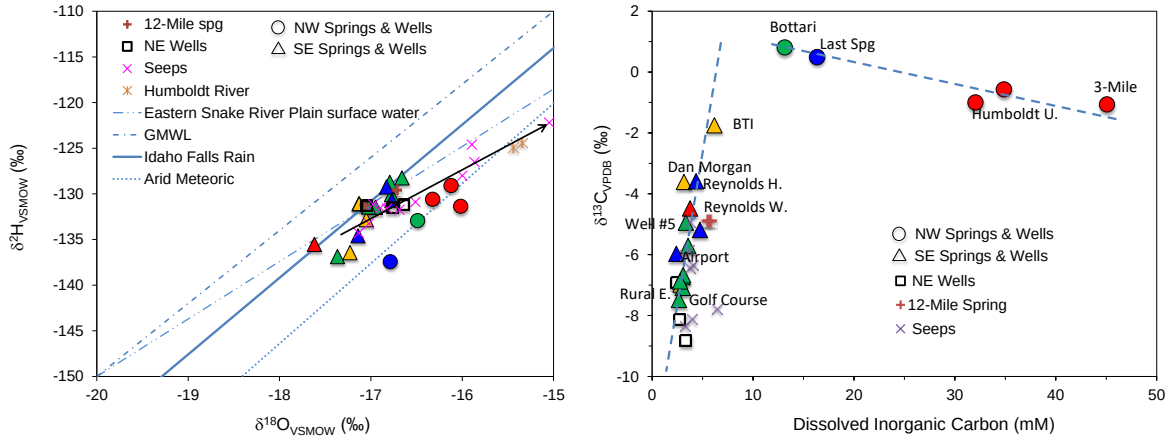

Figure 6. Plot of hydrogen versus oxygen isotopic compositions (left) and carbon isotopic composition versus dissolved inorganic carbon (right), showing distinct trends of waters from the Northwest Group (circles) and East Group (triangles and squares). Points shown as NE Wells in the legend (squares) correspond to the Richie's, Trap Range, and Windmill wells (see Figure 3 for locations). Points shown as Seeps in the legend correspond to seeps 1-11 in Figure 3; these seeps and Humboldt River samples follow an evaporation trend (arrow). Symbol colors indicate temperature as shown on the legend of Figure 4. GMWL stands for Global Meteoric Water Line. The line for Idaho Falls rain is from Rightmire and Lewis (1987), for the Eastern Snake River Plain surface water from Wood and Low (1986), and for arid meteoric climate from Welch and Preissler (1986).

5. NEW TEMPERATURE AND GEOPHYSICAL SURVEYS

In November, 2016 the City of Wells commissioned Zehner Geologic Consulting, LLC to perform a shallow, 2-m temperature survey (see Coolbaugh et al., 2007; Zehner et al., 2011) in the area around the city. Temperatures were measured at 1.0, 1.5, and 2.0 m below ground level at 73 sites across the project area. Temperatures at 14 of the sites were measured at or above background levels (13.0°C). Indications of weak, western-directed thermal outflow were detected adjacent to the Snake Mountains range front in the vicinity of the hot springs. Two sites east of the range front near Sulphur Hot Spring indicate that thermal upflow may occur along structures adjacent to the range front. The most interesting discovery from this survey was the identification of a strong thermal anomaly (Figures 1 and 7) along the northern edge of the Humboldt River due south of Sulphur Hot Spring. The anomaly is approximately 650 meters long with temperatures reaching 24.5°C at 2-m depth. Results from this survey were submitted in January 2017 to Elko Heat Company and the City of Wells in an unpublished report (Zehner, 2017a).

A direct-push Geoprobe survey was conducted on April 27, 2017 along the thermal anomaly identified by the shallow temperature survey (Figure 7). The Geoprobe was chosen as an inexpensive verification method to measure temperatures and obtain water samples at depths greater than the 2-m temperature survey. Eight un-cased holes ranging from 5 to 9 m in depth were advanced into the subsurface through unconsolidated sediments. Measured bottom-hole temperatures were between 32.2° and 45.4°C, indicative of a high geothermal gradient that could indicate the presence of geothermal fluids at shallow depths. The circulation of these hot fluids could result either from upflow along a fault mapped by Jewell (1982) and confirmed by new mapping (Figure 7) (Zuza, 2017), a south-directed outflow zone from the hot springs to the north, or some combination of the two. Results from this survey were submitted in May 2017 to Elko Heat Company and the City of Wells in an unpublished report (Zehner, 2017b). Subsequent to the April 2017 survey,

a few additional Geoprobe holes were advanced in June 2017 to the southwest and southeast of the thermal anomaly, although revealing lower temperatures than the April survey. No fluid samples were obtained from any of the Geoprobe holes.

Two complementary, near-surface geophysical methods (electromagnetic induction and direct current resistivity) were used to explore the shallow subsurface in the Wells study area. In July 2017, an electromagnetic induction (EMI) survey was deployed by NETL to determine the near-surface (~1–10 m) apparent conductivity of in the zone of anomalous subsurface temperatures (Figure 7). A second EMI survey was performed by NETL in proximity to Threemile Spring to investigate the conductivity contrast between thermal waters and unwetted soils on either side of the flowing geothermal surface outflow from this spring. At this location, near-surface geothermal waters were found to be expressed as a low conductivity anomaly in contrast with arid soils where salts are evaporatively concentrated. Using this rationale as a guide for geothermal prospecting, two areas of low conductivity were identified as potential geothermal targets along an elongated area of high conductivity on the north side of the Humboldt River (Figure 7). Zones of high conductivity were found to spatially correspond to upper terraces with sparse vegetation on both sides of the Humboldt River.

To probe greater depths than possible with the EMI surveys, three direct current (DC) resistivity profiles were acquired by NETL on the north side of the Humboldt River in September 2017 (Figures 7 and 8). Each DC resistivity survey made use of different electrode spacings (2, 3, and 4 m) and different array configurations.

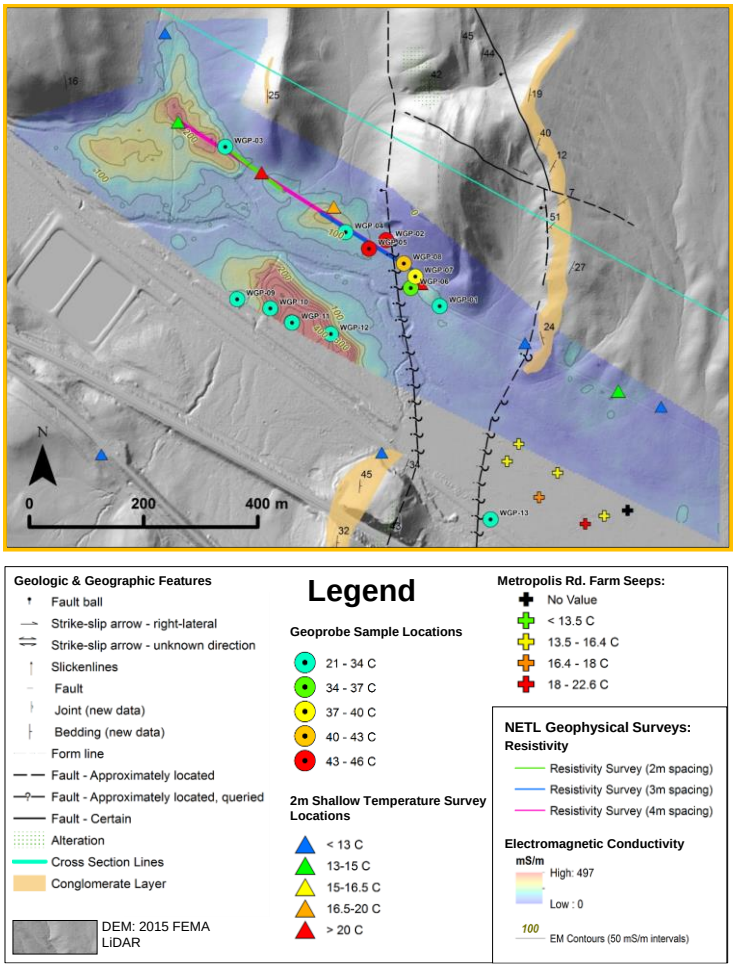

Figure 7. LiDAR map (courtesy FEMA, 2015) showing geologic details, temperature measurements, and geophysical data collected during field surveys for this study. The 3m and 4m spacing resistivity profiles are shown on Figure 8.

The resistivity/depth model depicts a near-surface zone of low resistivity (high conductivity), approximately 4-m thick that is present in the intervals x= 0 – 134 m and 168 – 348 m (Figure 8, top). This agrees with the location of conductive areas in the EMI conductivity map and is interpreted to represent the evaporative concentration of salts in the vadose zone. Beneath the near-surface conductive layer is a resistive layer of varying thickness (typically 2 to 4-m thick) that is present across the 444-m-long profile. Beneath this resistive layer is a discontinuous conductive layer that is notable for its extremely low resistivity in certain areas that suggest a porous material

containing highly conductive pore fluids. A highly resistive body can be seen in the lower portion of the 4-m resistivity/depth model that is presumed to be bedrock, including an area showing an unusually shaped, resistive pinnacle interpreted as a bedrock high (Figure 8, top). A DC resistivity survey with 3-m electrode spacing was conducted to improve the resolution of this zone (Figure 8, bottom). The location of this resistive pinnacle coincides with a normal fault inferred from geologic mapping (see dashed fault on Figure 7).

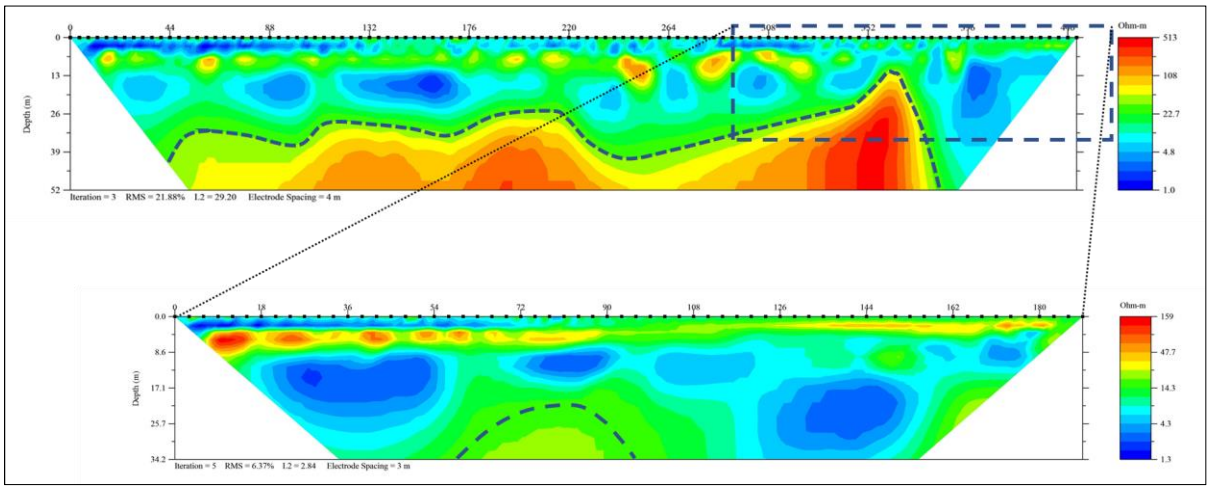

Figure 8. DC resistivity profile collected at 4-m electrode spacing (top) and shorter DC resistivity profile acquired at 3-m electrode spacing (bottom) using dipole-dipole arrays. The approximate area of the 3-m profile is shown as a dashed rectangle on the 4-m array profile. Note that the depth of exploration and resistivity color scale is different for each profile. A dashed line shows the inferred top of bedrock in both profiles.

6. DATA INTEGRATION AND GEOLOGIC MODEL DEVELOPMENT

All datasets collected for this study were cataloged, categorized, and compiled by NETL into an interactive summary document (a data catalog) shared as a public resource on NETL's Energy Data eXchange (EDX). EDX is a data-driven, web-based portal designed to encourage collaboration and science-based decision making. The data catalog primarily describes spatial datasets, and records dataset names, descriptions, categories, spatial extent, year published, formats, number of records, sources, citations, public availability, who acquired the dataset, and year the dataset was acquired. Using ESRI's ArcGIS software, the collected datasets were integrated into a geodatabase. In total, 47 individual spatial datasets were compiled into a single geodatabase. The integrated datasets included all historical and new geological/structural, geochemical, and geophysical data, as well as lithologic logs of all thermal and cold wells drilled in the study area available through the Nevada Division of Water Resources (NDWR) and the State of Nevada Commission on Mineral Resources, Division of Minerals (NDOM). Datasets were acquired in different formats, levels of completeness, and spatial reference systems, and needed to be converted to a format suitable for the geodatabase. All datasets also needed to be checked for the consistent spatial reference system information, duplication, and location errors in order to be imported into the final geodatabase. The data catalog and geodatabase are available for download at https://edx.netl.doe.gov/dataset/city-of-wells-geothermal-data.

A conceptual three-dimensional geologic model was built to visualize the three-dimensional datasets in geologic context. This model was constructed using EarthVision 9.1 (Dynamic Graphics, Inc.). Because of the heterogeneity of the sedimentary layers at the scale of the model, and lack of detail on many driller's logs, sedimentary horizons were incorporated, but not interpolated, into the 3-D model space. However, new well-logs (graphically illustrated from historical NDWR driller's logs) and cross-sections (Zuza, 2017; NETL, this study) were incorporated to inform the model as much as possible and to provide subsurface temperature data. Also, depth to basement was constrained using existing geophysical data and well log recordings.

Subsurface temperatures were modeled in three dimensions using the iterative "minimum tension gridding" algorithm native to EarthVision (Figure 9). This was achieved in several stages. First, individual temperature measurements were imported as scattered data and converted into a coarse 3-dimensional grid. Temperatures were assigned to grid nodes using an inverse-distance weighting average function. Next, several iterations were executed to calculate new temperature values for each grid node, with the neighboring nodes and scattered data informing a cubic function that assigns the new value. Once the initial set of iterations was completed for the coarse grid, temperatures were re-calculated for a new, finer-scale grid with user-defined dimensions. In addition, to better understand and visualize data density and quality, an uncertainty analysis was completed using the Cumulative Spatial Impact Layers (CSIL) geospatial tool developed by NETL (Bauer et al., 2015). This tool incorporates spatial datasets and summarizes them based on spatial overlap (presence or absence), which results in a dataset density feature layer for the area of interest. For the City of Wells geothermal investigation, a CSIL analysis was performed to represent the uncertainty of the geologic and geophysical datasets included in the 3-dimensional

geologic model. To further constrain the uncertainty of the 3-dimensional temperature model, a 3-dimensional point density analysis was also performed using the compiled wells and springs temperature data.

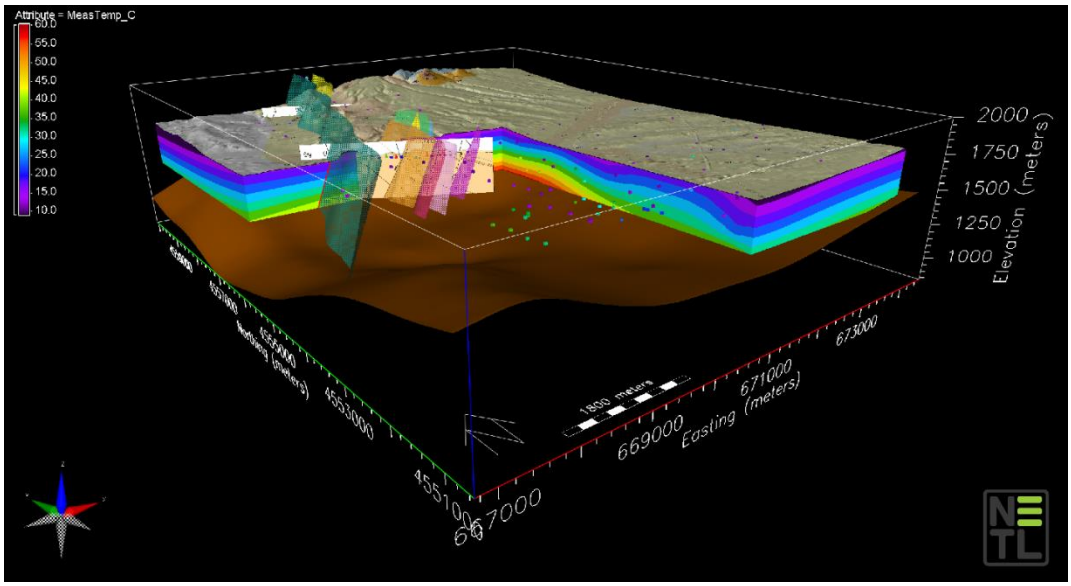

Figure 9. 3-D temperature model of the Wells, Nevada region (vertical exaggerations = 2). Temperature is modeled from red (hotter) to purple (cooler). Individual temperature data points are small colored boxes scattered throughout the model space. Fault planes that are colored and transparent intersect the model. Independently drawn cross-sections from Zuza (2017) were inserted within the temperature model for comparison. The newly mapped geology of the Wells region (Zuza, 2017) is also draped on the surface of the model along with the LiDAR DEM.

7. CONCLUSIONS

Geothermal upwelling is occurring along parts of the north-northeast-striking fault system on the west side of the Snake Mountains. Thermal springs and shallow temperature anomalies seem to coincide with the intersection of these faults with west-northwest-striking faults and fractures. The lower end of deep reservoir temperatures of the geothermal system(s) were estimated to be ~160°C, sufficient not only for district heating, but also for electricity generation. The highest water discharge temperatures (up to 53°C) were measured in the hot springs several kilometers north of town, too far away to economically pipe water to a district heating system in town. Exploration has therefore focused on areas along the Humboldt River and adjacent to a north-northeast-striking fault system that are much closer to town.

A shallow thermal anomaly was identified along the north side of the Humboldt River floodplain. This area coincides with the possible intersection of north-northeast- and (concealed) west-northwest-striking faults. Alternatively, this thermal anomaly could represent lateral geothermal outflow along permeable horizons coming from the hot spring area to the north.

Different chemical and isotopic signatures were identified in thermal waters along and west of the Snake Mountains range-bounding fault (Northwest group) compared to thermal waters east of this boundary (East Group). The composition of Northwest Group waters suggest a deeper origin, including older waters having a longer residency time, than for the East Group. No subsurface waters could be sampled within the shallow thermal anomaly and therefore it is unknown whether thermal fluids at this location belong to the Northwest or East group of waters or a mixing of the two. The low electrical resistivity measured in the shallow subsurface (depths < 50 m) in this area suggests the presence of either low-porosity rock such as claystones and siltstones and/or higher porosity material with warmer temperatures. The resistivity measurements also suggest a resistive feature at a depth of ~15 m which could be a silicified fault, perhaps the same fault observed above the floodplain escarpment to the north in the maps of Jewell (1982) and Zuza (2017) (Figure 7).

On the basis of this information, the City of Wells undertook the drilling of a shallow geothermal exploration borehole at the location of the hottest shallow temperature readings, as identified by the 2-meter shallow temperature and Geoprobe surveys. This location was also selected because it could provide evidence for either shallow hydrothermal outflow from the north, or for upflow along the east side of the western-most fault shown on Figure 7. The exploratory borehole (GEO #1) was drilled by air-rotary to a depth of 107 m by Rosenlund Drilling, LLC, between October 23 and November 1, 2017. This borehole did not reveal the expected level of locally elevated temperatures (maximum of ~ 23°C), potentially raising questions about the accuracy of the nearby Geoprobe temperature measurements, which were significantly higher (up to ~ 45°C). Other than a thin sandstone unit between 4 and 7 m depth, higher porosity rocks were not encountered in this borehole and up-flow of thermal waters was not evidenced. An interpretation of these results is that thermal waters at this location are limited to lateral flow along the thin, shallow sandstone unit encountered in GEO #1, from a

location further north closer to the hot springs. Also, only siltstone was encountered at greater depths, suggesting that the more electrically conductive rock visible on the DC resistivity profiles correspond to clay-rich siltstone rather than the sought-after higher porosity rock encompassing warmer waters. Another air-rotary exploratory borehole in the same area (GEO #2) was subsequently drilled to a similar depth (104 m) by the City of Wells in early January 2018. This borehole encountered water in a thin permeable zone at 12 m with maximum temperatures (~32°C) at 13 m depth; circulation was lost in fractures at greater depths, until the borehole penetrated clays at about 100 m depth. This appears to confirm the hypothesis of quite shallow thermal outflow at this location, however not warm enough nor in quantities significant enough for large-scale direct use applications. For this reason, further investigations are now focusing at greater depths in areas east of the faults shown on Figure 7. Another exploratory borehole (GEO #4) was drilled by mud-rotary in January 2018 to a depth of 213 m about mid-point between the shallow temperature anomaly and the Reynolds well; this borehole encountered temperatures up to 41°C at a depth of about 140 m (with noticeable water entry) then reversing to cooler temperatures at greater depths. The temperatures measured in these new boreholes are shown in Figure 10. For comparison, temperatures reported on the driller's logs of the warmest existing wells (BTI and Reynolds wells) and on the geophysical log of the Dalton #1 oil exploration well (Jewel, 1982) are also shown on Figure 10. Although none of these temperatures can be considered fully equilibrated, these data suggest that one should expect finding a resource suitable for direct use at moderate depths. The present study under the U.S. Department of Energy's Small Business Vouchers Pilot (SBV) Program will provide a basis for further investigations towards this goal.

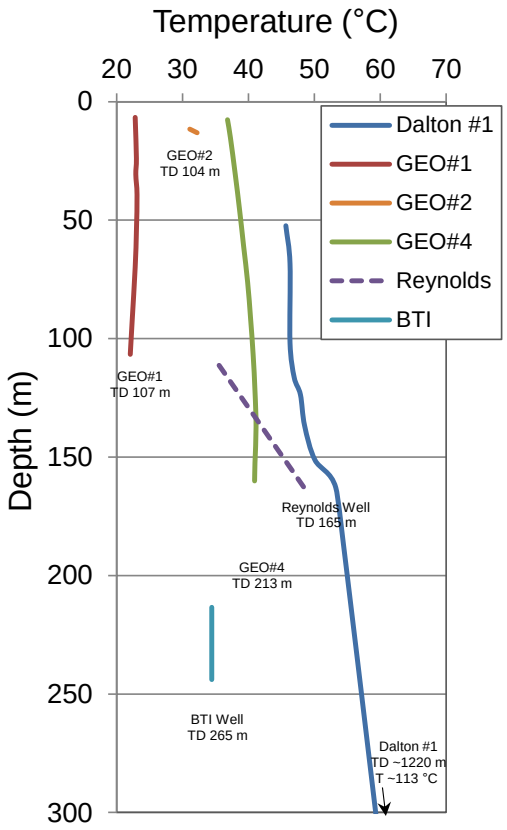

Figure 10. Temperatures measured in new exploratory boreholes (GEO #1, #2, and #4), existing warmest water wells (BTI and Reynolds wells), and the Dalton #1 oil exploration well (Jewel, 1982).

ACKNOWLEDGEMENTS

This work was supported by the U.S. Department of Energy, Office of Energy Efficiency and Renewable Energy (EERE), Office of Technology Development, Geothermal Technologies Program, under Award Number DE-AC02-05CH11231. We greatly appreciate the support of the U.S. Department of Energy's Small Business Vouchers Pilot (SBV) Program, without which this study could not have been undertaken. We thank local land owners for allowing access for mapping and sampling, and FEMA Flood Hazard Mapping for the preliminary LiDAR data. We also thank Paul Jewell for generously sharing unpublished water chemistry data from the Wells area, and are also grateful to Wenming Dong at LBNL for analyzing the concentrations of metals and anions in collected water samples.

REFERENCES

Bauer, J. R., Nelson, J., Romeo, L., Eynard, J., Sim, L., Halama, J., Rose, K., Graham, J. A.: Spatio-Temporal Approach to Analyze Broad Risks and Potential Impacts Associated with Uncontrolled Hydrocarbon Release Events in the Offshore Gulf of Mexico, *EPAct Technical Report Series*, NETL-TRS-2-2015, U.S. Department of Energy, National Energy Technology Laboratory: Morgantown, WV, (2015), 60p.

Bloomquist, R.G.: Elko Heat Company District Heating System – A case study. GeoHeat Center Bulletin, June, (2004), 7-10.

Coolbaugh, M.F., Sladek, C., Faulds, J.E., Zehner, R.E., and Oppliger, G.L.: Use of Rapid Temperature Measurements at a 2-meter Depth to Augment Deeper Temperature Gradient Drilling, *Proceedings, 32nd Workshop on Geothermal Reservoir Engineering*, Stanford University, Stanford, CA, Jan. 22-24, (2007), 109-116.

Evans J., and Derry L.A.: Quartz Control of High Germanium/Silicon Ratios in Geothermal Waters, *Geology*, **30** (11), (2002), 1019-1022.

Garside, L.J.: Geology of the Bishop Creek area, Elko County, Nevada, *Unpublished Masters Thesis*, University of Nevada, Reno, (1968).

Garside, L. J. and Schilling, J. H.: Thermal waters of Nevada, *Nevada Bureau of Mines and Geology Bulletin*, **91**, (1979), 163 p.

Garside, L.J.: Nevada Low-Temperature Geothermal Resource Assessment: 1994, Final Report prepared for the Oregon Institute of Technology Geoheat Center, *Nevada Bureau of Mines and Geology*, (1994), DOE/ID/13223-75.

Giggenbach, W.F.: Geothermal Solute Equilibria: Derivation of Na–K–Mg–Ca Geoindicators, *Geochim. Cosmochim. Acta*, **52**, (1988,) 2749-2755.

Henry, C.D., and Colgan, J.P.: The regional structural setting of the 2008 Wells earthquake and Town Creek Flat Basin — Implications for the Wells earthquake fault and adjacent structures. *Nevada Bureau of Mines and Geology Special Publication*, **36**, (2011), 53-64.

Henry, C.D., and Thorman, C.H.: Geologic map of the Wells area, Elko County, Nevada, *Nevada Bureau of Mines and Geology Special Publication*, **36**, (2011), Appendix A.

Jewell, P.W.: Geology and geothermal potential north of Wells, Nevada, *University of Utah Research Institute, Earth Science Laboratory*, Open File Report DOE/ID/12079-83, (1982), 38 p.

Jewell, P.W., Rahn, T.A., and Bowman, J.R.: Hydrology and Chemistry of Thermal Waters Near Wells, Nevada, *Ground Water*, **32** (4), (1994), 657-665.

Peiffer, L., Wanner, C., Spycher, N., Sonnenthal, E.L., Kennedy, B.M., and Iovenitti, J.: Multicomponent vs. classical geothermometry: insights from modeling studies at the Dixie Valley geothermal area, *Geothermics*, **51** (2014), 154-169.

Ponce, D.A., Watt, J.T., and Bouligand, C.: Geophysical setting of the February 21, 2008 Mw 6.0 Wells earthquake, Nevada, Implications for earthquake hazards, *Nevada Bureau of Mines and Geology Special Publication*, **36**, (2011), 89-100.

Reed, M.H., Spycher, N.F.: Calculation of pH and Mineral Equilibria in Hydrothermal Waters with Application to Geothermometry and Studies of Boiling and Dilution, *Geochim. Cosmochim. Acta*, **48**, (1984),1479-1492.

Ramelli, A.R., and dePolo, C.M.: Quaternary Faults in the 2008 Wells Earthquake Area, *Nevada Bureau of Mines and Geology Special Publication*, **36**, (2011), 79-88.

Rightmire C.T., Lewis B.D.: Hydrogeology and geochemistry of the unsaturated zone, radioactive waste management complex, Idaho National Engineering Laboratory, Idaho, *U.S. Geological Survey Water-Resources Investigations Report* 87-4198, (1987).

Sladek, C.: Effects on Geothermal Features Following the February 21, 2008 Wells, Nevada Earthquake, *Nevada Bureau of Mines and Geology Special Publication*, **36**, (2011), 377-384.

Smith, G.I., Friedman, I., Veronda, G., and Johnson, C.A.: Stable Isotope Compositions of Waters in the Great Basin, United States. 3. Comparison of Groundwaters with Modern Precipitation, *Journal of Geophysical Research*, **107** (D19), (2002), 4402, doi:10.1029/2001JD000567.

Smith, K., Pechmann, J., Meremonte, M., and Pankow, K.: Preliminary Analysis of the Mw 6.0 Wells, Nevada, Earthquake Sequence, *Nevada Bureau of Mines and Geology Special Publication*, **36**, (2011), 127-145.

Spycher, N., Peiffer, L., Sonnenthal, E.L., Saldi, G., Reed, M.H., and Kennedy, B.M.: Integrated Multicomponent Solute Geothermometry, *Geothermics*, **51**, (2014), 113-123.

Spycher N., Finsterle S., and Dobson, P.: New Developments in Multicomponent Geothermometry, *Proceedings*, 41st Workshop on Geothermal Reservoir Engineering Stanford University, Stanford, California, February 22-24, (2016), SGP-TR-209.

Thorman, C.H., Brooks, W.E., Ketner, K.B., and Dubiel, R.F.: Preliminary Geologic Map of the Oxley Peak area, Humboldt County, Nevada, *Nevada Bureau of Mines and Geology*, Open-File Report 2003-04, (2010).

Welch, A.H., Preissler, A.M.: Aqueous Geochemistry of the Bradys Hot Springs Geothermal Area, Churchill County, Nevada. In Selected Papers in the Hydrologic Sciences (S. Subitzky, Editor). *U.S. Geological Survey Water-Supply Paper* 2290, (1986).

Wood W.W., and Low, W.H.: Aqueous Geochemistry and Diagenesis in the Eastern Snake River Plain Aquifer System, Idaho, *Geological Society of America Bulletin*, **97**, (1986), 1456-1466.

Zehner, R.: Desktop Study of Geothermal Potential in and Around the City of Wells. Unpublished Report for The City of Wells and Better City, *Geothermal Development Associates*, (2016), 9p.

Zehner, R.: Shallow (2-Meter) Temperature Survey in and Around the City of Wells, Nevada: Implications for Geothermal Exploration, Unpublished Report for Elko Heat Company and The City of Wells, *Geothermal Development Associates*, (2017), 12p.

Zehner, R.: Shallow (2-Meter) Results of Geoprobe Survey Performed Within the Thermal Anomaly Identified by Shallow Temperature Survey Near Wells, Nevada, Unpublished Report for Elko Heat Company and The City of Wells, *Geothermal Development Associates*, (2017b), 8p.

Zehner, R.E., Tullar, K.N., and Rutledge, E.: Effectiveness of 2-Meter and Geoprobe Shallow Temperature Surveys in Early Stage Geothermal Exploration, *Geothermal Resources Council Transactions*, **36**, (2012), 835-841.

Zuza, A.V.: Preliminary Geologic Map of the Southern Snake Mountains Near Wells, Nevada, University of Nevada, Reno, *Nevada Bureau of Mines and Geology*, (2017).